Original Article

Institution of MECHANICAL ENGINEERS

Journal of SYSTEMS AND CONTROL ENGINEERING

Proc IMechE Part I: J Systems and Control Engineering
1–14

DOI: 10.1177/0959651817750521
journals.sagepub.com/home/pii
SAGE

Third-order leader-following consensus protocol of traffic flow formed by cooperative vehicular platoons by considering time delay: constant spacing strategy

Hossein Chehardoli and MR Homaeinezhad

Abstract
In this article, the problem of third-order consensus of homogeneous traffic flow formed by cooperative vehicular platoons is studied. This article is presented in two main parts. Inter-platoon stability analysis and intra-platoon stability analysis. For inter-platoon stability analysis, due to great length of traffic flow, it is assumed that lead vehicle is not available. Therefore, a new consensus algorithm based on bidirectional virtual leader-following strategy is introduced. Both communication and parasitic delays are involved in control design and stability analysis. By decoupling the closed-loop dynamics of cooperative leaders and employing the cluster treatment characteristic root method, necessary conditions on control parameters and stable regions of time delay satisfying internal stability of leaders' network are derived. In continuance of this part, inter-platoon string stability is studied. In the second part, it is assumed that the communication topology of each platoon is generic. Therefore, some of the eigenvalues of network matrix are complex which complicates the intra-platoon stability analysis. After decoupling the closed-loop dynamics of each platoon, a new consensus algorithm is presented. It will be shown that by this algorithm, the control parameters are independent of eigenvalues of network matrix which simplifies the controller design and stability analysis. Several simulation results are provided to show the effectiveness of the proposed approaches.

Keywords
Internal stability, string stability, decoupling, time delay, complex eigenvalue, cluster treatment characteristic root

Date received: 29 August 2017; accepted: 26 November 2017

Introduction

In recent decades, the problem of traffic congestion as an important environmental, economical, and social issue has received a lot of attentions.[1–3] The idea of intelligent transportation systems (ITS) is a useful policy to decrease the impact of traffic congestion, shorten travel time, and increase safety and lower fuel consumption.[4,5] The main idea of ITS is to control the autonomous vehicles to constitute the cooperative platoons in which all platoons move with identical velocity and as small as possible inter-platoon and intra-platoon spacing.[5] Therefore, the traffic capacity and fuel efficiency will increase.

The coordinated motion of a group of vehicles with the same velocity and small inter-vehicles spacing is called vehicular platooning.[5–7] The vehicular platooning has received much attention since 1980s.[5] Due to employing smaller inter-vehicle spacing compared with typical adaptive cruise controls, vehicular platooning has a significant potential to achieve and implement the idea of ITS.[5,8] In implementing vehicular platooning, three important indexes are considered.[9] Internal stability has the same concept as asymptotic stability, string stability, and scalability. A vehicular platoon is said to be internal stable if all the roots of the closed-loop dynamics locate on the left-hand side of imaginary axis.[10,11] The string stability assures that the spacing

Department of Mechanical Engineering, K. N. Toosi University of Technology, Tehran, Iran

Corresponding author:
Hossein Chehardoli, Department of Mechanical Engineering, K. N. Toosi University of Technology, P. O. Box: 19395-1999, Tehran 1999143344, Iran.
Email: hchehardoli@gmail.com

errors will not propagate along the platoon when a disturbance signal is applied to lead vehicle's motion.[12] The scalability studies the effect of platoon size on stability margin of closed-loop dynamics.[13]

The control structure of an autonomous vehicle is composed of two levels: (1) upper level controller and (2) lower level controller. The upper level controller calculates the desired value of acceleration and lower level controller calculates the appropriate inputs for the throttle and brake actuators to produce the desired acceleration specified by the upper level controller.[14]

To adjust the inter-vehicle spacing, two general strategies are employed in platooning control: (1) constant spacing strategy (CSS)[6] and (2) constant time headway strategy (CTHS).[11] In CTHS, the inter-vehicular spacing is a function of velocity. But in the CSS, it is controlled to remain constant. A vehicular platoon is called homogeneous if all vehicles have identical dynamics. Otherwise, it is heterogeneous.[10]

A great deal of research studies have been done on stability analysis and control design of vehicular platooning. These works can be categorized from several aspects of view. Centralized controller schemes are studied by Santini et al., Chehardoli and Homaeinezhad, and Naus et al.,[8,10,12,15] and decentralized controllers are investigated by Santhana and Rajamani, Ghasemi et al., Khatir and Davidson, and Ploeg et al.[6,11,16,17] In the works by Chehardoli and Homaeinezhad and Bernardo et al.,[10,18,19] second-order consensus of vehicular platoons is studied, whereas different third-order linear consensus protocols are presented in the works by Ghasemi et al., Naus et al., Zheng et al., and Chehardoli and Homaeinezhad.[11–13,15] In the works by Chehardoli and Homaeinezhad, Middleton and Braslavsky, and Ghasemi et al.,[19–21] it is assumed that all vehicles in platoon are homogeneous. The internal and string stability analysis of heterogeneous platoons is studied by Chehardoli and Homaeinezhad, Wang and Nijmeijer, and Bernardo et al.[10,22,23] Several linear control protocols are provided by Chehardoli and Homaeinezhad, Khatir and Davidson, Ghasemi et al., and Peters et al.,[10,16,21,24] whereas different nonlinear schemes are presented by Guo et al., Swaroop et al., and Kwon and Chwa.[25–27] A robust control based on sliding mode controller is presented in the work by Swaroop et al.[26] to guarantee the internal and string stability of homogeneous vehicular platoons with second-order dynamics. A new adaptive control scheme is presented by Guo et al. and Kwon and Chwa[25,27] to estimate the uncertain parameters such as rolling resistance and air drag coefficient. In the works by Santhana and Rajamani, Ghasemi et al., and Bernardo et al.[6,11,18,23] and Chehardoli and Homaeinezhad, Naus et al., Swaroop et al., and Ghasemi and Rouhi,[10,12,26,28] CTHS and CSS are employed to adjust the inter-vehicle spacing. Due to vehicle-to-vehicle (V2V) and vehicle-to-infrastructure (V2I) communication, time delay is attracted much more attention to vehicular platooning.[10,12,15,23,24] In the works by Naus et al. and Peters et al.,[12,24] communication delay is considered homogeneous, whereas in the works by Chehardoli and Homaeinezhad and Bernardo et al.,[10,15,23] it is assumed heterogeneous. The safety and collision avoidance problem is discussed widely in the works by Chehardoli and Homaeinezhad and Ghasemi and Rouhi.[15,28] In the work by Ghasemi et al.,[11] by employing partial differential equation (PDE) approximation, the closed-loop dynamics of vehicular platoons is decoupled. However, due to limitation of this approach, communication and parasitic delays cannot be modeled by PDE approximation. A new uncertain leader-following consensus algorithm is presented in the work by Wu et al.[29,30] to stabilize the closed-loop dynamics of multi-agent systems.

To the best of our knowledge, despite huge amount of relevant literature to date (of which a large part was addressed in the previous paragraph), the stability analysis and control design for the whole of traffic flow have not been studied so far. In practical implementations, a traffic flow consists of cooperative vehicular platoons in which leaders exchange information with each other. A traffic flow consists of two different cooperative networks: (1) lead vehicles' communication network which is called inter-platoon network and (2) the communication network of individual platoons which is called intra-platoon network. All the previous studies focused on stability of intra-platoon network. In this article, the stability analysis of traffic flow as the combination between cooperative vehicular platoons is investigated.

Due to the great length of traffic flow, the leader of inter-platoon network may be not available. Also, it is assumed that each leader in inter-platoon network is in communication with preceding and subsequent leaders. Therefore, the inter-platoon network topology is bidirectional virtual leader-following (BDVLF) topology. A new consensus protocol is defined for inter-platoon network and it will be shown that without the position information of virtual leader, both inter-platoon internal and string stability are guaranteed. By employing the cluster treatment characteristic root (CTCR) method, the stable regions of communication and parasitic delays for inter-platoon network are calculated.

The intra-platoon network is assumed to be non-uniform and generic. Therefore, some eigenvalues of network may be complex which makes the stability analysis more difficult. In previous works on networks with generic topology, the control parameters are strictly dependent on network's eigenvalues. This makes the controller design more complicated, especially when the communication topology is varying by time. Therefore, in this article, a new approach based on decoupling of intra-platoon closed-loop dynamics is introduced rectifying this problem.

In summary, the main contributions of this article are as follows:

1. Introducing a new virtual leader-following scheme based on CSS to guarantee both inter-platoon

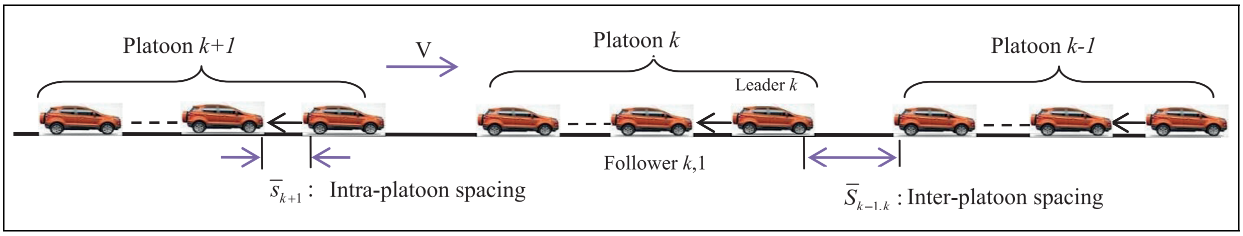

Figure 1. A traffic flow as the combination of cooperative platoons.

internal and string stability in the presence of communication and parasitic delays.

2. Introducing a new control protocol by decoupling the intra-platoon closed-loop dynamics in which the control parameters are independent on network structure.

The rest of this article is organized as follows: in section "Graph theory," a brief review of graph theory is presented. In section "Stability analysis of lead vehicles' network," inter-platoon internal and string stability analyses are studied. In section "Intra-platoon stability analysis," intra-platoon stability analysis is presented. In section "Simulation studies," several simulation results are provided to show the effectiveness of the proposed methods. Finally, section "Conclusion" concludes the article. Also, some applicable lemmas and theorems are listed in Appendices 1 and 2.

Graph theory

Let $G=(V,E,\mathbf{A})$ is a graph of order N with $V=\{1,2,...,N\}$ which represents node set, $E\subseteq N\times N$ is the set of edges, and $\mathbf{A}$ is the adjacency matrix with nonnegative elements. An edge (i,j) denotes that the node j has access to the information of the node i. Set of neighbors of node i is shown by $N_i=\{j\in V:(j,i)\in \varepsilon, j\neq i\}$. In the leader–follower scheme, for the follower agents 1 to N, there exists a leader labeled by 0. Information is exchanged between the leader and the follower agents which belong to the neighbors of the leader. Then, the graph $\bar{G}=(\bar{V},\bar{E},\mathbf{A})$ with node set $\bar{V}=V\cup\{0\}$ and edge set $\bar{E}=\bar{V}\times\bar{V}$ represents the communication topology between the leader and the followers. A diagonal matrix $\mathbf{B}\in\Re^{N\times N}$ is defined as a leader adjacency matrix of $\bar{G}$ with diagonal elements $b_i=a_{i0}$. If lead vehicle is a neighbor of vehicle i, $a_{i0}>0$ and $a_{i0}=0$, otherwise. Node 0 is globally reachable in $\bar{G}$ if there is a path form every node $i\in V$ to it. For graph G, the Laplacian matrix $\hat{\mathbf{L}}=[\hat{l}_{ij}]\in\Re^{N\times N}$ is defined with $\hat{l}_{ii}=\sum_{j=1,\neq i}^{N}a_{ij}$ and $\hat{l}_{ij}=-a_{ij}$, $i\neq j$. Also, for graph $\bar{G}$, the important matrix $\mathbf{H}=\hat{\mathbf{L}}+\mathbf{B}$ is defined.

Stability analysis of lead vehicles' network

In this section, the inter-platoon internal and string stability of homogeneous traffic flow is considered. Figure 1 shows the homogeneous traffic flow as the combination of cooperative vehicular platoons.

Internal stability of lead vehicles' network

Due to great length of traffic flow, the communication topology of leaders' network is assumed to be BDVLF topology. Each leader is in communication with its neighbors and virtual leader through V2V and V2I communication. The longitudinal motion of leader i is described by the following linear differential equation[11–13,15]

$$\varsigma\dot{a}_{0,i}+a_{0,i}=u_{0,i} \tag{1}$$

where ς, $a_{0,i}$, and $u_{0,i}$ are time constants of engine, acceleration, and control input, c, the virtual leader-following consensus protocol is defined as follows

$$\begin{aligned} u_{0,i}(t)=\sum_{j=1}^{N_{0,i}}a_{ij}\big[&\alpha_2\big(J(d_{0,ij})-v_{0,i}(t)\big)\\ &+\alpha_3\big(v_{0,j}(t-\tau_{0,ij})-v_{0,i}(t)+a_l(t-\tau_l)\tau_{0,ij}\big)\big]\\ &+\alpha_1\big(v_{0,i}(t)-v_l\big) \end{aligned} \tag{2}$$

where $\alpha_1,\alpha_2,\alpha_3$ are positive control gains (the procedure of calculating these parameters is introduced in Theorem 1); v_l,a_l are the velocity and the acceleration of virtual leader; $N_{0,i}$ is the number of neighbors of ith leader; $v_{0,i}$ is the velocity of leader i; $\tau_{0,ij},\tau_l$ are V2V and V2I communication delays; and $d_{0,ij}$ is defined as follows

$$d_{0,ij}=\frac{1}{i-j}\left(x_{0,j}(t-\tau_{0,ij})-x_{0,i}-\sum_{k=j}^{i-1}\sum_{r=1}^{N_k}(L_{k,r}+\bar{s}_k)+\sum_{r=j}^{i-1}\bar{S}_r+v_l(t-\tau_l)\tau_{0,ij}\right) \tag{3}$$

where $x_{0,j}()$ denotes the position of leader j and $L_{k,r},\bar{s}_k,\bar{S}_k$ are the length of vehicle r in platoon k, constant intra-platoon spacing of platoon k, and constant inter-platoon spacing between consecutive platoons. Also, the function $J(d_{0,ij})$ is defined as follows

$$J(d_{0,ij})=\frac{\bar{v}}{2}\left(1+\tanh\left(2\pi\frac{d_{0,ij}-\frac{R_1+R_2}{2}}{R_2-R_1}\right)\right) \tag{4}$$

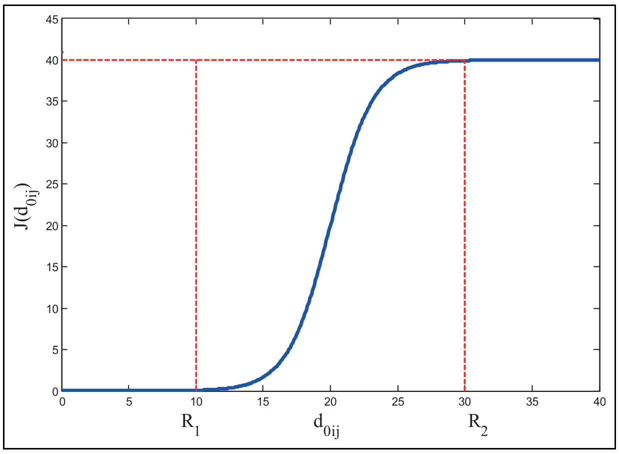

Figure 2. Range policy function J.

where $R_1, R_2, \bar{v}$ are positive constants. Figure 2 shows the range policy function $J()$ for selected values $R_1 = 10\,\mathrm{m}$, $R_2 = 30\,\mathrm{m}$, and $\bar{v} = 40\,\mathrm{m/s}$. This range spacing policy function assures the safety of inter-platoon network and increases the traffic capacity. If $d_{0,ij} < R_1$, the leaders tend to brake to avoid the collision and if $d_{0,ij} > R_2$, leaders reach to $\bar{v}$, to decrease the inter-platoon spacing.

Based on CSS, the inter-platoon error and its time derivatives are defined in the following form

$$e_{0,i} = x_{0,i} - x_l + \sum_{k=1}^{i-1}\sum_{r=1}^{N_k}(L_{k,r} + \bar{s}_k) + \sum_{r=j}^{i-1}\bar{S}_r,\ \dot{e}_{0,i} = v_{0,i} - v_l,\ \ddot{e}_{0,i} = a_{0,i},\ \dddot{e}_{0,i} = \dot{a}_{0,i} \tag{5}$$

where x_l is the position of virtual leader. It should be noted that since the leader is virtual, x_l does not have a physical meaning and is not employed in controller design. Replacing equations (2), (3), and (5) in equation (1) and assuming that $v_l = J(d_{0,ij}(t_0))$ and $v_l(t-\tau_l) \approx v_l(t)$, the closed-loop dynamics of leader i will be in the following form

$$\varsigma\,\dddot{e}_{0,i} + \ddot{e}_{0,i} = \sum_{j=1}^{N_{0,i}} a_{ij}\left[\frac{\alpha_2}{i-j}J(d_{0,ij}(t_0))\big(e_{0,j}(t-\tau_{0,ij}) - e_{0,i}\big) + \alpha_3\dot{e}_{0,j}(t-\tau_{0,ij}) - (\alpha_1+\alpha_2)\dot{e}_{0,i}(t)\right] + \alpha_1\dot{e}_{0,i} \tag{6}$$

Equation (6), by adding the effect of parasitic delay (δ), will be in the following form

$$\varsigma e_{0,i} + \ddot{e}_{0,i} = \sum_{j=1}^{N_{0,i}} a_{ij}\left[\frac{\alpha_2}{i-j}J(d_{0,ij}(t_0))\big(e_{0,j}(t-\bar{\tau}_{0,ij}) - e_{0,i}(t-\delta)\big) + \alpha_3\dot{e}_{0,j}(t-\bar{\tau}_{0,ij}) - (\alpha_2+\alpha_3)\dot{e}_{0,i}(t-\delta)\right] + \alpha_1\dot{e}_{0,i}(t-\delta) \tag{7}$$

where $\bar{\tau}_{0,ij} = \tau_{0,ij} + \delta$. For BDVLF topology, equation (7) will be in the following form

$$\begin{aligned}\varsigma\dddot{e}_{0,i} + \ddot{e}_{0,i} &= \alpha_2 J'(d_{0,ij}(t_0))\\ &(e_{0,i-1}(t-\bar{\tau}_{0,i,i-1}) - e_{0,i}(t-\delta)) + \alpha_2 J'(d_{0,ij}(t_0))\\ &(e_{0,i+1}(t-\bar{\tau}_{0,i,i+1}) - e_{0,i}(t-\delta))\\ &+ (\alpha_1 - 2(\alpha_2+\alpha_3))\dot{e}_{0,i}(t-\delta)\\ &+ \alpha_3\dot{e}_{0,i-1}(t-\bar{\tau}_{0,i,i-1}) + \alpha_3\dot{e}_{0,i+1}(t-\bar{\tau}_{0,i,i+1})\end{aligned} \tag{8}$$

For leaders' network, the error vector is defined as $\mathbf{E} = [e_1, \dot{e}_1, \ddot{e}_1, \ldots, e_N, \dot{e}_N, \ddot{e}_N]$. Therefore, the inter-platoon closed-loop dynamics is in the following form

$$\dot{\mathbf{E}}(t) = \mathbf{I}_N \otimes \mathbf{C}_1\mathbf{E}(t) + \mathbf{A}\otimes\mathbf{C}_2\mathbf{E}(t-\bar{\tau}_{ij}) + \mathbf{I}_N\otimes\mathbf{C}_3\mathbf{E}(t-\delta) \tag{9}$$

where

$$\mathbf{C}_1 = \begin{pmatrix} 0 & 1 & 0\\ 0 & 0 & 1\\ 0 & 0 & -1/\varsigma\end{pmatrix},$$

$$\mathbf{C}_2 = \begin{pmatrix} 0 & 0 & 0\\ 0 & 0 & 0\\ \alpha_2 J'(d_{0,ij}(t_0))/\varsigma & \alpha_3/\varsigma & 0\end{pmatrix},$$

$$\mathbf{C}_3 = \begin{pmatrix} 0 & 0 & 0\\ 0 & 0 & 0\\ z_1/\varsigma & z_2/\varsigma & 0\end{pmatrix},$$

$$\mathbf{A} = \begin{pmatrix} 0 & 1 & 0 & \ldots & 0 & 0\\ 1 & 0 & 1 & \ldots & 0 & 0\\ \vdots & \vdots & \vdots & \vdots & \vdots & \vdots\\ 0 & 0 & 0 & \ldots & 1 & 0\end{pmatrix}$$

and $z_1 = -2\alpha_2 J(d_{0,ij}(t_0))$, $z_2 = \alpha_1 - 2(\alpha_2+\alpha_3)$. For the inter-platoon adjacency matrix $\mathbf{A}$, there exist matrices $\mathbf{T}$ and $\mathbf{\Xi}$ such that $\mathbf{T}^{-1}\mathbf{A}\mathbf{T} = \mathbf{\Xi}$, where $\mathbf{\Xi}$ is a diagonal matrix of eigenvalues of matrix $\mathbf{A}$. By defining $\mathbf{E} = (\mathbf{T}\otimes\mathbf{I}_3)\boldsymbol{\xi}$, equation (9) can be written in the following form

$$\begin{aligned}\dot{\boldsymbol{\xi}} &= (\mathbf{T}^{-1}\otimes\mathbf{I}_3)(\mathbf{I}_N\otimes\mathbf{C}_1)(\mathbf{T}\otimes\mathbf{I}_3)\boldsymbol{\xi}(t)\\ &+ (\mathbf{T}^{-1}\otimes\mathbf{I}_3)(\mathbf{A}\otimes\mathbf{C}_2)(\mathbf{T}\otimes\mathbf{I}_3)\boldsymbol{\xi}(t-\bar{\tau}_{0,ij})\\ &+ (\mathbf{T}^{-1}\otimes\mathbf{I}_3)(\mathbf{I}_N\otimes\mathbf{C}_3)(\mathbf{T}\otimes\mathbf{I}_3)\boldsymbol{\xi}(t-\delta)\end{aligned} \tag{10}$$

By applying Lemma 5 to equation (10), we will have the following

$$\dot{\boldsymbol{\xi}} = (\mathbf{I}_N\otimes\mathbf{C}_1)\boldsymbol{\xi}(t) + (\mathbf{\Lambda}\otimes\mathbf{C}_2)\boldsymbol{\xi}(t-\bar{\tau}_{0,ij}) + (\mathbf{I}_N\otimes\mathbf{C}_3)\boldsymbol{\xi}(t-\delta) \tag{11}$$

So that the decoupled forms of equation (9) are as follows

$$\dot{\boldsymbol{\xi}}_i = \mathbf{C}_1\boldsymbol{\xi}_i(t) + \lambda_i\mathbf{C}_2\boldsymbol{\xi}_i(t - \bar{\tau}_{0,ij}) + \mathbf{C}_3\boldsymbol{\xi}_i(t - \delta) \tag{12}$$

where λ_i is ith eigenvalue of matrix $\mathbf{A}$. In the work by Ghasemi et al.,[11] by employing the PDEs, the intra-platoon closed-loop dynamics is decoupled. But, due to limitation of this approach, time delay is not considered. Due to great distance between leaders, the communication delay should be considered in system modeling and control design.

Theorem 1. The decoupled equation (12) without time delay is globally asymptotically stable under the following conditions

$$J'(d_{0,ij}(t_0)) > 0,\ \alpha_1 < 2\alpha_2,\ \alpha_3 > \varsigma\alpha_2 J'(d_{0,ij}(t_0)) \tag{13}$$

Proof. The characteristic equation of equation (12) without considering delay is in the following form

$$\varsigma s^3 + s^2 - (\lambda_i\alpha_3 + z_2)s - (z_1 + \lambda_i\alpha_2 J'(d_{0,ij}(t_0))) = 0 \tag{14}$$

By employing Routh–Hurwitz criterion, it is shown that under the following conditions, equation (14) is stable

$$\begin{aligned} &z_1 + \lambda_i\alpha_2 J'(d_{0,ij}(t_0)) < 0 \Rightarrow (\lambda_i - 2)J'(d_{0,ij}(t_0)) < 0,\\ &(2 - \lambda_i)\big(\alpha_3 - \varsigma\alpha_2 J'(d_{0,ij}(t_0))\big) - \alpha_1 + 2\alpha_2 > 0 \end{aligned} \tag{15}$$

For the range policy function (4), it can be easily shown that $J'(d_{0,ij}(t_0)) > 0$. From Gershgorin theorem,[31] it is inferred that $|\lambda_i| \leqslant 2$. Therefore, it can be easily checked that under conditions (equation (13)), all inequalities of equation (15) are satisfied.

To calculate the stable regions of time delay, the CTCR method is employed.[32] The characteristic equation of equation (12) is in the following form

$$\begin{aligned} ce_i = s\mathbf{I}_3 - \mathbf{C}_1 - \mathbf{C}_2\lambda_i e^{-\bar{\tau}s} - \mathbf{C}_3 e^{-\delta s} \Rightarrow ce_i = \varsigma s^3\\ + s^2 - \lambda_i(\alpha_3 s + \alpha_2 J'(0))e^{-\bar{\tau}s} - (z_1 + z_2 s)e^{-\delta s} \end{aligned} \tag{16}$$

Since ce_i has infinite roots, the stability analysis by applying Routh–Hurwitz method to equation (16) is impossible. Therefore, the following exact Rekasius transformations are introduced[32]

$$e^{-\bar{\tau}s} = \frac{1 - T_1 s}{1 + T_1 s},\ e^{-\delta s} = \frac{1 - T_2 s}{1 + T_2 s},\ s = j\omega,\ \omega \in \Re^+ \tag{17}$$

The imaginary roots of equation (16) remain invariant under Rekasius transformation.[32] By considering $s = j\omega$, defining $\sigma_1 = T_1\omega$, $\sigma_2 = T_2\omega$ and replacing equation (17) in equation (16), ce_i will be in the following form

$$ce_i = \sum_{k=0}^{3} m_k\omega^k + j\sum_{k=0}^{3} n_k\omega^k \tag{18}$$

where

$$\begin{aligned} &m_0 = -(z_1 + \alpha_2\lambda_i)\sigma_1\sigma_2 - (z_1 + \lambda_i\alpha_2 J'(0)),\\ &m_1 = (z_2 + \lambda_i\alpha_3)(\sigma_2 - \sigma_1),\ m_2 = \sigma_1\sigma_2 - 1,\\ &m_3 = \varsigma(\sigma_1 + \sigma_2)\\ &n_0 = (\sigma_1 - \sigma_2)(z_1 + \lambda_i\alpha_2),\\ &n_1 = -(\lambda_i\alpha_3 + z_2)\sigma_1\sigma_2 - z_2 - \lambda_i\alpha_3,\\ &n_2 = -(\sigma_1 + \sigma_2),\ n_3 = -\varsigma(\sigma_1\sigma_2 + 1) \end{aligned} \tag{19}$$

To exist imaginary roots for equation (16), both real and imaginary parts of equation (18) must be zero simultaneously. If Sylvester's matrix associated with equation (18) is singular, there exist imaginary roots for equation (16). Sylvester's matrix associated with equation (18) is in the following form

$$\mathbf{M}_s = \begin{pmatrix} m_3 & m_2 & m_1 & m_0 & 0 & 0\\ 0 & m_3 & m_2 & m_1 & m_0 & 0\\ 0 & 0 & m_3 & m_2 & m_1 & m_0\\ n_3 & n_2 & n_1 & n_0 & 0 & 0\\ 0 & n_3 & n_2 & n_1 & n_0 & 0\\ 0 & 0 & n_3 & n_2 & n_1 & n_0 \end{pmatrix} \tag{20}$$

We can express that

$$\det(\mathbf{M}_s) = F(\sigma_1, \sigma_2) = F(\tan(0.5\delta\omega), \tan(0.5\bar{\tau}\omega)) = 0 \tag{21}$$

which constitutes a closed-form description of the kernel curves in the spectral delay space (SDS) $(\delta, \bar{\tau})\omega$.[32] Every point $(\delta\omega, \bar{\tau}\omega)$ on SDS brings an imaginary characteristic root at $\pm j\omega$. Using the transformation $(\tau, \delta) = 2(\tan^{-1}(\tau, \delta) \pm k\pi)/\omega$, $k = 0, 1, 2, \ldots,$ the kernel and offspring hypercurves are derived from SDS diagram.[32] For an imaginary root $s = j\omega$, the root tendency is defined as follows[32]

$$RT|_{s=j\omega}^{\tau_j} = \operatorname{sgn}\left[\operatorname{Re}\left(\left.\frac{\partial s}{\partial\tau}\right|_{s=j\omega}\right)\right] \tag{22}$$

If the root tendency is positive, by increasing the value of one delay (while other delays are constant), the imaginary root $s = j\omega$ will be unstable. Using kernel and offspring hypercurves and the concept of root tendency, the stable regions of time delay for characteristic equation (16) are obtained. More details about CTCR method can be found in the work by Ergenc et al.[32]

String stability of leaders' network

Taking Laplace transform of both sides of equation (8) leads to

$$E_i(s) = \Gamma_{i-1}(s)E_{i-1}(s) + \Gamma_{i+1}(s)E_{i+1}(s)$$
$$\Gamma_{i-1} = \frac{(\alpha_2 J'(d_{0,ij}(t_0)) + \alpha_3 s)e^{-\bar{\tau}s}}{\varsigma s^3 + s^2 + (2(\alpha_2+\alpha_3)-\alpha_1)se^{-\delta s} + 2\alpha_2 J'(0)e^{-\delta s}},$$
$$\Gamma_{i+1} = \frac{(\alpha_2 J'(d_{0,ij}(t_0)) + \alpha_3 s)e^{-\bar{\tau}s}}{\varsigma s^3 + s^2 + (2(\alpha_2+\alpha_3)-\alpha_1)se^{-\delta s} + 2\alpha_2 J'(0)e^{-\delta s}} \tag{23}$$

where $E_i(s)$ is the Laplace transform of $e_i(t)$ and $\bar{\tau} = \max_{i,j}(\bar{\tau}_{ij})$. By doing some algebraic manipulations, we have

$$\frac{E_i}{E_{i-1}} = \frac{\Gamma_{i-1}}{1-\Gamma_{i+1}(E_{i+1}/E_i)} \tag{24}$$

Theorem 2. The inter-platoon network is string stable under the following condition

$$[\alpha_1 - 2(\alpha_2+\alpha_3)]^2 + 8\alpha_2 J'(d_{0,ij}(t_0))\alpha_1\delta - 4\alpha_2 J'(d_{0,ij}(t_0))[1+4(\alpha_2+\alpha_3)]\delta > 0 \tag{25}$$

Proof. According to equation (24), if the conditions $|\Gamma_{i-1}(j\omega)|$, $|\Gamma_{i+1}(j\omega)| \leqslant 0.5$ and $|E_N(j\omega)/E_{N-1}(j\omega)| \leqslant 1$ are met, then $|E_i(j\omega)/E_{i-1}(j\omega)| \leqslant 1$. Consider $|\Gamma_{i-1}| = \sqrt{\bar{p}_{i-1}/\bar{q}_{i-1}} \leqslant 1/2 \Rightarrow \bar{q}_{i-1} - 4\bar{p}_{i-1} \geqslant 0$. Where

$$\begin{aligned}\bar{p}_{i-1} &= \varsigma^2\omega^6 + \omega^4 + (2(\alpha_2+\alpha_3)-\alpha_1)^2\omega^2 \\ &\quad - 2(2(\alpha_2+\alpha_3)-\alpha_1)\varsigma\omega^4\cos\delta\omega \\ &\quad - 4(2(\alpha_2+\alpha_3)-\alpha_1)\omega\alpha_2 J'(d_{0,ij}(t_0))\sin(2\delta\omega) \\ &\quad + 4\omega^3\varsigma\alpha_2 J'(d_{0,ij}(t_0))\sin\delta\omega \\ &\quad - 4\omega^2\alpha_2 J'(d_{0,ij}(t_0))\cos\delta\omega \\ &\quad + 4\omega^3(2(\alpha_2+\alpha_3)-\alpha_1)\sin\delta\omega + 4\alpha_2^2 J'^2(d_{0,ij}(t_0)) \\ \bar{q}_{i-1} &= {\alpha_2}^2 J'^2(d_{0,ij}(t_0)) + {\alpha_3}^2\omega^2\end{aligned}$$

By performing some algebraic manipulations, the inequality $\bar{q}_{i-1} - 4\bar{p}_{i-1} \geqslant 0$ is simplified to follows

$$\begin{aligned}&\varsigma^2\omega^6 + \omega^4 + (2(\alpha_2+\alpha_3)-\alpha_1)^2\omega^2 \\ &\quad - 2(2(\alpha_2+\alpha_3)-\alpha_1)\varsigma\omega^4\cos\delta\omega \\ &\quad - 4(2(\alpha_2+\alpha_3)-\alpha_1)\omega\alpha_2 J'(d_{0,ij}(t_0))\sin(2\delta)\omega \\ &\quad + 4\omega^3\varsigma\alpha_2 J'(d_{0,ij}(t_0))\sin\delta\omega \\ &\quad - 4\omega^2\alpha_2 J'(d_{0,ij}(t_0))\cos\delta\omega \\ &\quad + 2\omega^3(2(\alpha_2+\alpha_3)-\alpha_1)\sin\delta\omega - 4\alpha_3^2 \geqslant 0\end{aligned} \tag{26}$$

According to the following math expressions

$$\forall\vartheta \geqslant 0 : \sin\vartheta \leqslant \vartheta \to -\sin\vartheta \geqslant -\vartheta,$$
$$\sin\vartheta \geqslant -\vartheta,\ \cos\vartheta \leqslant 1 \to -\cos\vartheta \geqslant -1$$

Equation (26) is simplified as follows

$$\begin{aligned}&\varsigma^2\omega^6 + \left[1 - (4(\alpha_2+\alpha_3)-2\alpha_1)\varsigma - 2\delta\varsigma\alpha_2 J'(d_{0,ij}(t_0)) - (4(\alpha_2+\alpha_3)-2\alpha_1)\delta\right]\omega^4 \\ &+ \left\{[\alpha_1 - 2(\alpha_2+\alpha_3)]^2 - 4\alpha_2 J'(d_{0,ij}(t_0))\delta(1+4(\alpha_2+\alpha_3)-2\alpha_1) - 4{\alpha_3}^2\right\}\omega^2 \geqslant 0\end{aligned} \tag{27}$$

Since spacing errors have most of their energy in the region of low frequency, this region is most determinant in string stability analysis.[33] Therefore, in equation (27), if the coefficient of ω^2 be positive, the string stability is assured. So that under condition (equation (25)), inequality (equation (27)) is satisfied. Performing the similar analysis for $|\Gamma_{i+1}| = \sqrt{\bar{p}_{i+1}/\bar{q}_{i+1}} \leqslant 1/2$, leads to the same result as equation (25). For the last vehicle, we have the following

$$E_N(s) = \Gamma_{N-1}(s)E_{N-1}(s),\ \Gamma_{N-1} = \frac{(\alpha_2 J'(d_{0,ij}(t_0)) + \alpha_3 s)e^{-\bar{\tau}s}}{\varsigma s^3 + s^2 + (\alpha_2+\alpha_3-\alpha_1)se^{-\delta s} + \alpha_2 J'(d_{0,ij}(t_0))e^{-\delta s}} \tag{28}$$

It can be easily shown that if equation (25) holds, then $|E_{N-1}(j\omega)/E_N(j\omega)| < 1$. Therefore, it is concluded that under condition (equation (25)), the inter-platoon string stability is assured.

Intra-platoon stability analysis

Intra-platoon internal stability under generic network topology

In some of previous studies, the intra-platoon network topology is assumed to be generic.[7,15,18,19,23,34–36] In most of the works,[7,8,10,15,18,19,23,37,38] some eigenvalues of network topology are complex which makes the stability analysis more complicated specially when the network topology is time-varying. In these studies, the control parameters are strictly dependent on network's eigenvalues. Motivated to this problem, by decoupling the closed-loop dynamics, a new leader-following consensus protocol is presented to overcome this difficulty. It will be shown that by the proposed approach, the control parameters are independent of the network topology.

The longitudinal model of vehicle i in platoon k can be represented as follows. In this section, $\bar{\mathbf{A}}$ and $\bar{\mathbf{B}}$ are adjacency matrices of following and lead vehicles, respectively

$$\dot{\mathbf{x}}_{i,k} = \bar{\mathbf{C}}_1\mathbf{x}_{i,k} + \bar{\mathbf{C}}_2 u_{i,k},\ \mathbf{x}_i = [x_i, v_i, a_i]^T,$$
$$\bar{\mathbf{C}}_1 = \begin{pmatrix} 0 & 1 & 0 \\ 0 & 0 & 1 \\ 0 & 0 & -1/\varsigma \end{pmatrix},\ \bar{\mathbf{C}}_2 = [0, 0, 1/\varsigma]^T \tag{29}$$

The following control scheme is considered for each vehicle

$$
\begin{aligned}
u_{i,k}(t) = (\mathbf{L}+\bar{\mathbf{L}})\bar{b}_i\Big[\mathbf{x}_{0,k}(t-\tau_{0i}) - \mathbf{x}_{i,k}(t) + (\tau_{0i}v_{0,k}(t-\tau_{0i}) - \bar{s}_{0,i})\hat{\mathbf{i}} + \tau_{0i}a_{0,k}(t-\tau_{0i})\hat{\mathbf{j}}\Big] \\
+ \mathbf{L}\sum_{j=1}^{N}\bar{a}_{ij}\Big[\mathbf{x}_{j,k}(t-\tau_{ij}) - \mathbf{x}_{i,k}(t) + \big(\tau_{ij}v_{0,k}(t-\tau_{ij}) - \bar{s}_{ij}\big)\hat{\mathbf{i}} + \tau_{ij}a_{0,k}(t-\tau_{ij})\hat{\mathbf{j}}\Big]
\end{aligned}
\tag{30}
$$

where $\mathbf{L} = [l_1, l_2, l_3]$, $\bar{\mathbf{L}} = [\bar{l}_1, \bar{l}_2, 0]$ are intra-platoon control gains; $\hat{\mathbf{i}} = [1,0,0]^T$, $\hat{\mathbf{j}} = [0,1,0]^T$, N is the length of platoon; and $\bar{s}_{0i}$ is the desired spacing between leader and ith vehicle which is defined as follows

$$d_{0,i} = \sum_{j=1}^{i}(\bar{s}_k + L_{j-1,k}) \tag{31}$$

where $\bar{s}_k$ is the constant spacing and $L_{j-1,k}$ is the length of preceding vehicle in platoon k. From equation (31), it is concluded that $\bar{s}_{ji} = \bar{s}_{0i} - \bar{s}_{0j}$. For vehicle i in platoon k, the error vector is defined as follows

$$\mathbf{e}_{i,k} = \mathbf{x}_{0,k} - \mathbf{x}_{i,k} - \bar{s}_{0i}\hat{\mathbf{i}} \tag{32}$$

By assuming that $a_{0,k}(t-\tau) \approx a_{0,k}(t)$ and $v_{0,k}(t-\tau) \approx v_{0,k}(t)$, the control law (equation (30)) in terms of error vector is expressed as follows

$$u_{i,k}(t) = (\mathbf{L}+\bar{\mathbf{L}})\bar{b}_i\mathbf{e}_{i,k}(t) + \mathbf{L}\sum_{j=1}^{N}\bar{a}_{ij}\big[\mathbf{e}_{i,k}(t) - \mathbf{e}_{j,k}\big(t-\tau_{ij}\big)\big] \tag{33}$$

Time derivative of both sides of equation (32), replacing equation (30) in it and considering parasitic delay (δ) yields the following

$$
\begin{aligned}
\dot{\mathbf{e}}_{i,k}(t) = \bar{\mathbf{C}}_1\mathbf{e}_{i,k}(t) - \bar{\mathbf{C}}_2(\mathbf{L}+\bar{\mathbf{L}})\bar{b}_i\mathbf{e}_{i,k}(t-\delta) \\
- \bar{\mathbf{C}}_2\mathbf{L}\sum_{j=1}^{N}\bar{a}_{ij}\big[\mathbf{e}_{i,k}(t-\delta) - \mathbf{e}_{j,k}\big(t-\bar{\tau}_{ij}\big)\big]
\end{aligned}
\tag{34}
$$

where $\bar{\tau}_{ij} = \tau_{ij} + \delta$. By defining $e_k = [e_{1,k}, e_{2,k}, \ldots, e_{N,k}]^T$, the closed-loop dynamics of platoon k in terms of tracking error will be written as follows

$$
\begin{aligned}
\dot{\mathbf{e}}_k(t) = \big(\mathbf{I}_N \otimes \bar{\mathbf{C}}_1\big)\mathbf{e}_k(t) - \big[\mathbf{\Delta} \otimes (\bar{\mathbf{C}}_2\mathbf{L}) + \mathbf{I}_N \otimes \big(\bar{\mathbf{C}}_2\bar{\mathbf{L}}\big)\big] \\
\mathbf{e}_k(t-\delta) + \sum_{i=1}^{N}\sum_{j=1}^{N}\big(\bar{\mathbf{A}}_{ij} \otimes (\bar{\mathbf{C}}_2\mathbf{L})\big)\mathbf{e}_k(t-\bar{\tau}_{ij})
\end{aligned}
\tag{35}
$$

where $a_{kl} = \begin{cases} h_{ij} & k=i, l=j \\ 0 & otherwise \end{cases}$, $\bar{\mathbf{A}}_{ij} = [a_{kl}]_{ij}$, $\mathbf{\Delta} = diag\{d_i + b_i\}$, d_i is the degree of node i, and h_{ij} is the element of matrix $\mathbf{H}$. A necessary (but not sufficient) condition for stability of system (35) is stability without delay. System (35) without considering time delay will be in the following form

$$\dot{\mathbf{e}}_k(t) = \big[\mathbf{I}_N \otimes \bar{\mathbf{C}}_c - \mathbf{H} \otimes \big(\bar{\mathbf{C}}_2\mathbf{L}\big)\big]\mathbf{e}_k(t) \tag{36}$$

where $\bar{C}_c = \begin{pmatrix} 0 & 1 & 0 \\ 0 & 0 & 1 \\ -\bar{l}_1 & -\bar{l}_2 & -1/\varsigma \end{pmatrix}$. Before presenting the main theorem, the following new theorem is proposed.

Theorem 3. It is assumed that $\mathbf{H}$ has n distinct real eigenvalues ε_i with the repetition order n_i and m distinct complex eigenvalues $\bar{\varepsilon}_i = p_i + jq_i$ with the repetition order m_i. So that $\sum_1^n n_r + \sum_1^m m_r = N$. There exists a non-singular matrix $\mathbf{V} \in \Re^{N\times N}$ such that

$$\mathbf{V}^{-1}\mathbf{H}\mathbf{V} = \mathbf{\Xi},\ \mathbf{\Xi} = diag(\mathbf{\Xi}_1, \ldots, \mathbf{\Xi}_n, \mathbf{\Xi}_{n+1}, \ldots, \mathbf{\Xi}_{n+m}) \tag{37}$$

where $\mathbf{\Xi}_i$, $i = 1, 2, \ldots, n+m$ are Jordan blocks associated with real and complex eigenvalues. For repetitive real eigenvalues, Jordan blocks are in the following form ($i = 1, \ldots, n$)

$$\Xi_i = \begin{bmatrix} \varepsilon_i & 1 & \ldots & 0 \\ 0 & \varepsilon_i & \ddots & \vdots \\ \vdots & \ddots & \ddots & * \\ 0 & \ldots & 0 & \varepsilon_i \end{bmatrix} \tag{38}$$

Based on nilpotent degree of $\varepsilon_i, * \in \{0,1\}$.[35] The Jordan blocks associated with $\bar{\varepsilon}_i$ are as follows ($i = n+1, \ldots, n+m$)

$$\mathbf{\Xi}_i = \begin{bmatrix} \bar{\mathbf{\Xi}}_i & \mathbf{I}_2 & & \\ 0 & \bar{\mathbf{\Xi}}_i & \ddots & \\ \vdots & \ddots & \ddots & \mathbf{I}_2 \\ 0 & \ldots & 0 & \bar{\mathbf{\Xi}}_i \end{bmatrix},\ \bar{\mathbf{\Xi}}_i = \begin{bmatrix} p_i & q_i \\ -q_i & p_i \end{bmatrix} \tag{39}$$

Proof. The proof of Theorem 3 is explained in Appendix 1.

Theorem 4. The system (36) under the following conditions is globally asymptotically stable

$$\mathbf{L} = \frac{\bar{\mathbf{C}}_2^T\mathbf{P}^{-1}}{2} \tag{40a}$$

where $\mathbf{P}$ is a positive definite matrix satisfying $\bar{\mathbf{C}}_c\mathbf{P} + \mathbf{P}\bar{\mathbf{C}}_c^T \prec \mathbf{0}$

$$\bar{l}_2 > \varsigma\bar{l}_1,\ l_2 > \varsigma l_1 \tag{40b}$$

Proof. According to Lemma 1, since lead vehicle is globally reachable in platoon, matrix $\mathbf{H}$ is positive definite. By defining $\mathbf{e}_k(t) = (\mathbf{V}\otimes\mathbf{I}_3)\bar{\boldsymbol{\xi}}_k(t)$ and employing Lemma 5, equation (36) can be written as follows

$$\dot{\bar{\boldsymbol{\xi}}}_k(t) = \left(\mathbf{V}^{-1}\otimes\mathbf{I}_3\right)\left[\mathbf{I}_N\otimes\bar{\mathbf{C}}_c - \mathbf{H}\otimes\left(\bar{\mathbf{C}}_2\mathbf{L}\right)\right](\mathbf{V}\otimes\mathbf{I}_3)\bar{\boldsymbol{\xi}}_k(t)$$
$$= \left(\mathbf{I}_N\otimes\bar{\mathbf{C}}_c - \boldsymbol{\Xi}\otimes\left(\bar{\mathbf{C}}_2\mathbf{L}\right)\right)\bar{\boldsymbol{\xi}}_k(t) = \mathbf{C}_c\boldsymbol{\xi}_k(t) \tag{41}$$

According to equations (38) and (39), we have the following

$$\mathbf{C}_c = \begin{pmatrix} \bar{\mathbf{C}}_c - \varepsilon_i\bar{\mathbf{C}}_2\mathbf{L} & -\bar{\mathbf{C}}_2\mathbf{L} & \mathbf{0} & \\ \mathbf{0} & \bar{\mathbf{C}}_c - \varepsilon_i\bar{\mathbf{C}}_2\mathbf{L} & \ddots & \mathbf{0} \\ \vdots & \mathbf{0} & \ddots & -{}^*\bar{\mathbf{C}}_2\mathbf{L} \\ \mathbf{0} & \cdots & \mathbf{0} & \bar{\mathbf{C}}_c - \varepsilon_i\bar{\mathbf{C}}_2\mathbf{L} \end{pmatrix},$$
$$i = 1, 2, \ldots, n \tag{42}$$

$$\mathbf{C}_c = \begin{pmatrix} \tilde{\mathbf{C}}_i & -\mathbf{I}_2\otimes(\bar{\mathbf{C}}_2\mathbf{L}) & \mathbf{0} & \\ \mathbf{0} & \tilde{\mathbf{C}}_i & \ddots & \mathbf{0} \\ \vdots & \mathbf{0} & \ddots & -\mathbf{I}_2\otimes(\bar{\mathbf{C}}_2\mathbf{L}) \\ \mathbf{0} & \cdots & \mathbf{0} & \tilde{\mathbf{C}}_i \end{pmatrix},$$
$$\tilde{\mathbf{C}}_i = \mathbf{I}_2\otimes\bar{\mathbf{C}}_c - \begin{pmatrix} p_i & q_i \\ -q_i & p_i \end{pmatrix}\otimes(\bar{\mathbf{C}}_2\mathbf{L}), \quad i = n+1, \ldots, n+m \tag{43}$$

System (41) is asymptotically stable if

$$\bar{\mathbf{C}}_c - \varepsilon_i\bar{\mathbf{C}}_2\mathbf{L} \prec \mathbf{0}$$
$$\tilde{\mathbf{C}}_i = \mathbf{I}_2\otimes\bar{\mathbf{C}}_c - \begin{pmatrix} p_i & q_i \\ -q_i & p_i \end{pmatrix}\otimes(\bar{\mathbf{C}}_2\mathbf{L}) \prec \mathbf{0} \tag{44}$$

For real eigenvalues, the characteristic equation of matrix $\bar{\mathbf{C}}_c - \varepsilon_i\bar{\mathbf{C}}_2\mathbf{L}$ is in the following form

$$\lambda^3 + \left(\frac{1}{\varsigma} + l_3\varepsilon_i\right)\lambda^2 + (\bar{l}_2 + \varepsilon_i l_2)\lambda + (\bar{l}_1 + \varepsilon_i l_1) = 0 \tag{45}$$

By employing Routh–Hurwitz criterion, it can be easily verified that if the following expression is satisfied, equation (44) is asymptotically stable

$$l_3\varepsilon_i\left(\bar{l}_2 + \varepsilon_i l_2\right) + \frac{1}{\varsigma}\left(\bar{l}_2 + \varepsilon_i l_2\right) - \left(\bar{l}_1 + \varepsilon_i l_1\right) > 0 \tag{46}$$

Since $\varepsilon_i > 0$, it is obvious that if $\bar{l}_2 > \varsigma\bar{l}_1$ and $l_2 > \varsigma l_1$, then $\bar{\mathbf{C}}_c - \varepsilon_i\bar{\mathbf{C}}_2\mathbf{L} \prec \mathbf{0}$. According to Lemma 3, if there is a positive definite matrix $\mathbf{P}$ satisfying the following expression, equation (44) is satisfied

$$\left(\mathbf{I}_2\otimes\bar{\mathbf{C}}_c - \begin{pmatrix} p_i & q_i \\ -q_i & p_i \end{pmatrix}\otimes(\bar{\mathbf{C}}_2\mathbf{L})\right)(\mathbf{I}_2\otimes\mathbf{P})$$
$$+ (\mathbf{I}_2\otimes\mathbf{P})\left(\mathbf{I}_2\otimes\bar{\mathbf{C}}_c^T - \begin{pmatrix} p_i & -q_i \\ q_i & p_i \end{pmatrix}\otimes(\mathbf{L}^T\bar{\mathbf{C}}_2^T)\right) \prec \mathbf{0} \tag{46}$$

Using Lemma 5, equation (46) will be as follows

$$\mathbf{I}_2\otimes\left(\bar{\mathbf{C}}_c\mathbf{P} + \mathbf{P}\bar{\mathbf{C}}_c^T\right) - \begin{pmatrix} p_i & q_i \\ -q_i & p_i \end{pmatrix}\otimes(\bar{\mathbf{C}}_2\mathbf{L}\mathbf{P})$$
$$- \begin{pmatrix} p_i & -q_i \\ q_i & p_i \end{pmatrix}\otimes\left(\mathbf{P}\mathbf{L}^T\bar{\mathbf{C}}_2^T\right) \prec \mathbf{0} \tag{47}$$

Under condition (equation (40a)), $\bar{\mathbf{C}}_c \prec \mathbf{0}$. Therefore, there exist positive definite matrices $\mathbf{P}, \mathbf{Q} \succ \mathbf{0}$ such that $\bar{\mathbf{C}}_c\mathbf{P} + \mathbf{P}\bar{\mathbf{C}}_c^T = -\mathbf{Q}$. By choosing $\mathbf{L} = \bar{\mathbf{C}}_2^T\mathbf{P}^{-1}/2$, equation (47) will be in the following form

$$\mathbf{I}_2\otimes\left(\bar{\mathbf{C}}_c\mathbf{P} + \mathbf{P}\bar{\mathbf{C}}_c^T\right) - \begin{pmatrix} p_i & 0 \\ 0 & p_i \end{pmatrix}\otimes\bar{\mathbf{C}}_2\bar{\mathbf{C}}_2^T$$
$$= \mathbf{I}_2\otimes\left(\bar{\mathbf{C}}_c\mathbf{P} + \mathbf{P}\bar{\mathbf{C}}_c^T - p_i\bar{\mathbf{C}}_2\bar{\mathbf{C}}_2^T\right) = -\mathbf{I}_2\otimes\bar{\mathbf{Q}} \tag{48}$$

According to Lemma 4, $\bar{\mathbf{Q}} \succ \mathbf{0}$. Therefore, the proof is complete.

Remark 1. In addition to CTCR method, the Razumikhin and Krasovskii theorems are also employed to stability analysis of time delay systems (for additional information, readers are referred to the works by Qiu and colleagues[39,40]). Also, the modeling of leader-following scheme of inter-platoon network via Markov chains is an interesting subject deserving some further investigations.[41,42]

Remark 2. Since the control methodologies provided in this article describes the procedure of upper level control, these methods also can be employed for all kinds of gasoline and electric ground vehicles.[43,44]

Simulation studies

In this section, a homogeneous traffic flow consisting of 10 cooperative vehicular platoons is investigated. The length of each platoon (number of following vehicles) is 10. In this section, time responses of leaders' network and platoon 7 are studied. Figure 3 shows the network structure of platoon 7 and Figure 4 depicts the SDS diagrams of inter-platoon network.

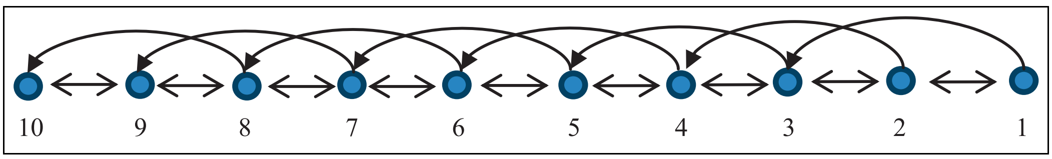

Figure 3. Network topology of platoon 7.

Table 1. Control gains and constant parameters.

$\alpha_2 = 4.1$	$\alpha_3 = 5.3$	$\alpha_1 = 8.7$	$\bar{s}_k = 10\,\mathrm{m}$	$\bar{S}_k = 25\,\mathrm{m}$
$\bar{\mathbf{L}} = [2, 4, 0]$	$R_1 = 10\,\mathrm{m}$	$R_2 = 20\,\mathrm{m}$	$\varsigma = 0.1$	$\bar{v} = 40\,\mathrm{m/s}$
$\delta = 0.11\,\mathrm{s}$	$\tau_l = 0.2$	$\tau_{0,i,i+1} = 0.22\,\mathrm{s}$	$\tau_{k,i,i+1} = 0.13\,\mathrm{s}$	$L = 4\,\mathrm{m}$

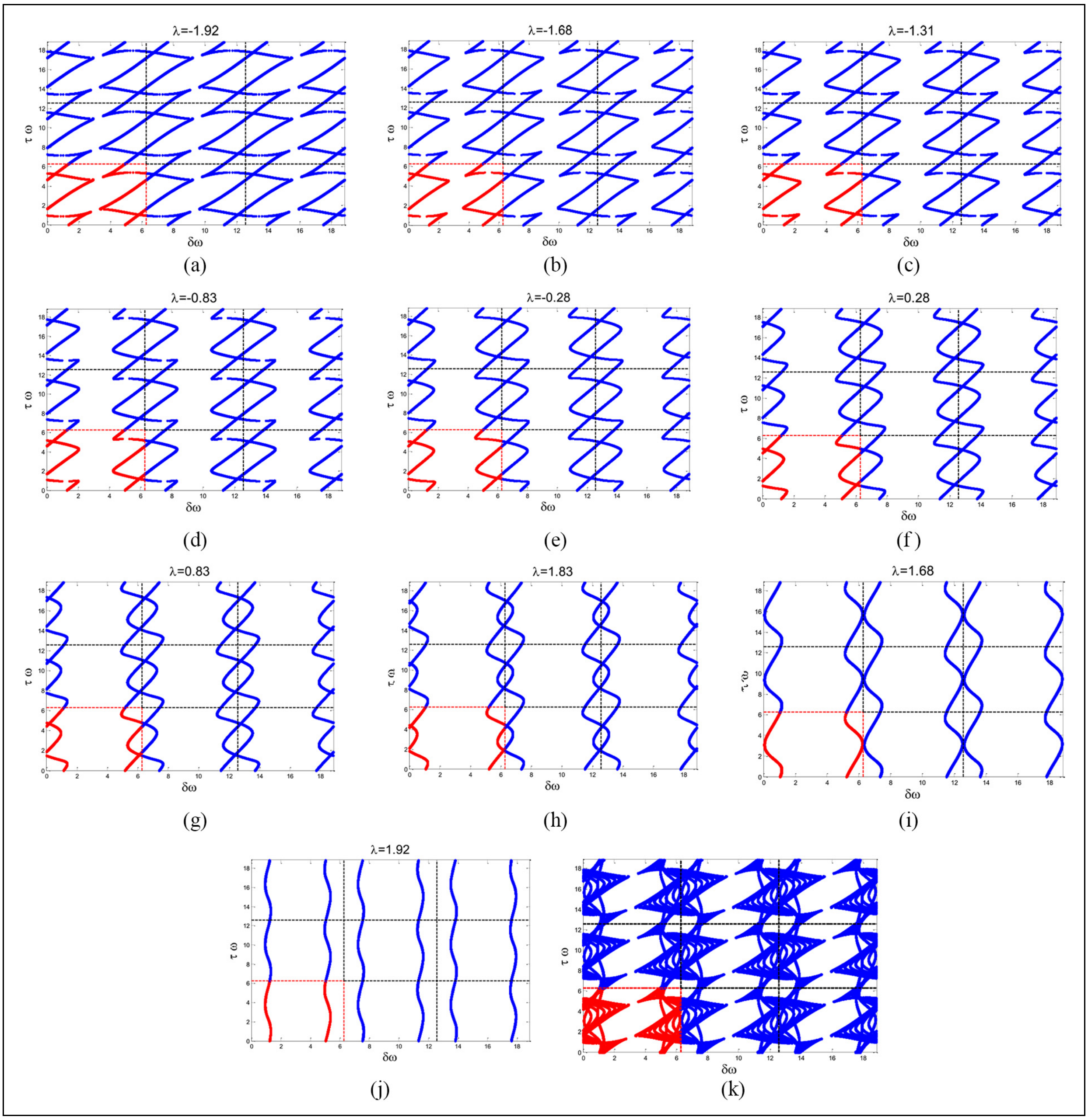

Figure 4. Spectral delay space for eigenvalues of leaders' adjacency matrix. (a) $\lambda = -1.92$, (b) $\lambda = -1.66$, (c) $\lambda = -1.31$, (d) $\lambda = -0.83$, (e) $\lambda = -0.28$, (f) $\lambda = -0.28$, (g) $\lambda = -0.83$, (h) $\lambda = 1.83$, (i) $\lambda = 1.68$, (j) $\lambda = 1.92$, (k) total SDS diagram.

The eigenvalues of matrix $\mathbf{H}$ of platoon 7 are as follows: 1, 1.58, 2.11, 2.83, 3.56, 5.31, $\pm 0.8j$, $4.99 \pm 0.36j$, 4.32. Table 1 shows the control gains and constant parameters used in the simulation studies.

Inter-platoon stability simulation

The CTCR method implementation. In the stability analysis of inter-platoon network, the spacing error is defined as $\Delta_{0,i} = x_{0,i-1} - x_{0,i} - d_{0ij}$. The control parameters

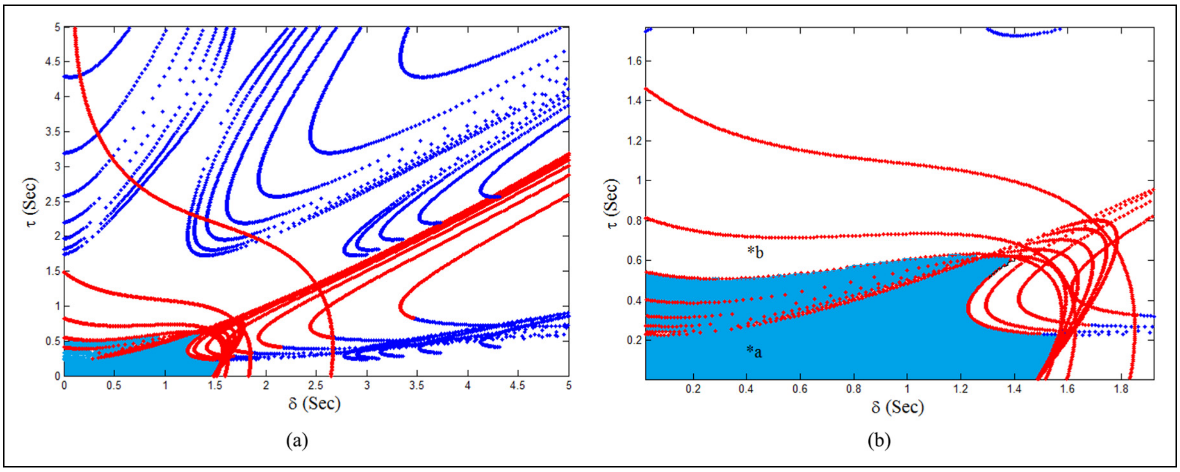

Figure 5. Stable region of communication and parasitic delays for leaders' network. (a) Kernel and offspring hypercurves, (b) Stable regions of communication and parasitic delays.

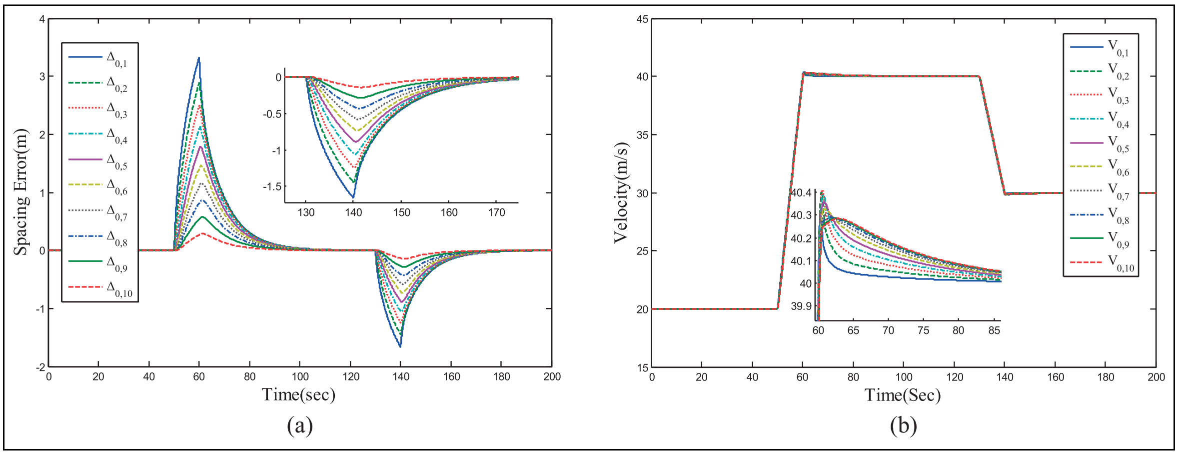

Figure 6. Behavior of lead vehicles' motion: point "a": (a) Spacing error of lead vehicles and (b) velocity of lead vehicles.

presented in Table 1 satisfy the conditions (equation (13)). In continuance, the stable regions of time delay are calculated by employing the CTCR method. At first, by employing equations (18)–(21), the SDS diagrams are obtained for each eigenvalues of inter-platoon adjacency matrix (Figure 4). Afterward, using the relation $(\tau, \delta) = 2\left(\tan^{-1}(\tau, \delta) \pm k\pi\right)/\omega$, $k = 0, 1, 2, \ldots,$ the kernel and offspring hypercurves are derived from SDS diagrams. Figure 5 shows the kernel and offspring hypercurves for inter-platoon network. The stable regions of time delay can be specified by calculating the root tendency (equation (22)). In Figure 5, the stable regions are specified.

Inter-platoon stability discussion. In order to verify the results, two different points "a" and "b" are considered which are inside and outside of the stable regions. Figure 6 shows the spacing error and velocity of lead vehicles for delays related to point "a." According to Figure 6(a), the inter-platoon internal stability is assured. Moreover, according to this figure, the amplitude of error decreases along the network indicating the string stability of inter-platoon network. Figure 7 shows the unstable behavior of inter-platoon network for delays related to point "b."

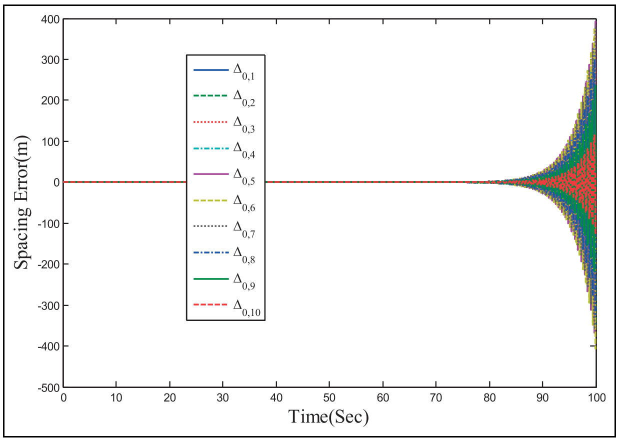

Figure 7. Inter-platoon unstable behavior: point "b."

Intra-platoon stability simulation

The intra-platoon spacing error is defined as $\Delta_i = x_{i-1} - x_i - L_{i-1} - \bar{s}$. To evalute the intra-platoon

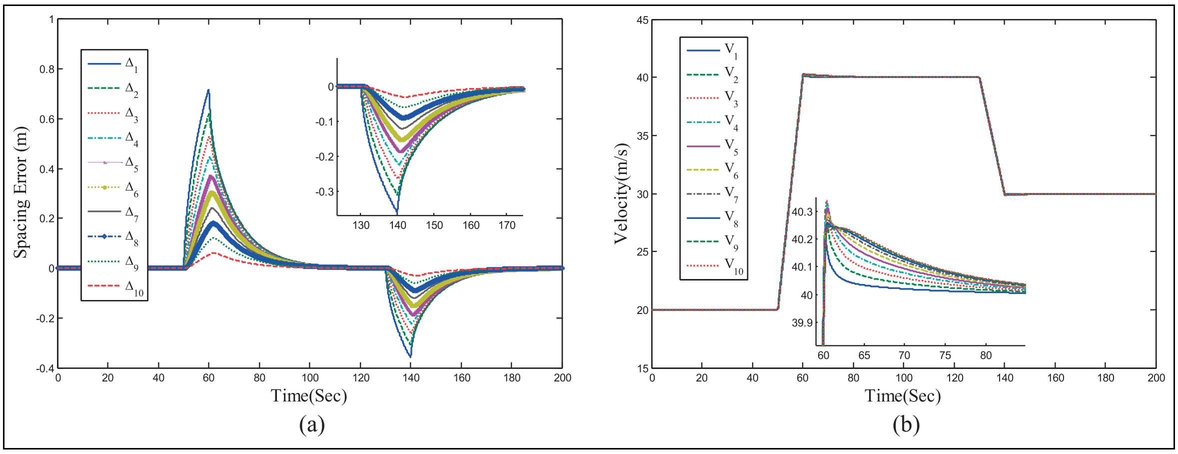

Figure 8. Behavior of vehicles in platoon 7: (a) spacing error and (b) velocity of vehicles.

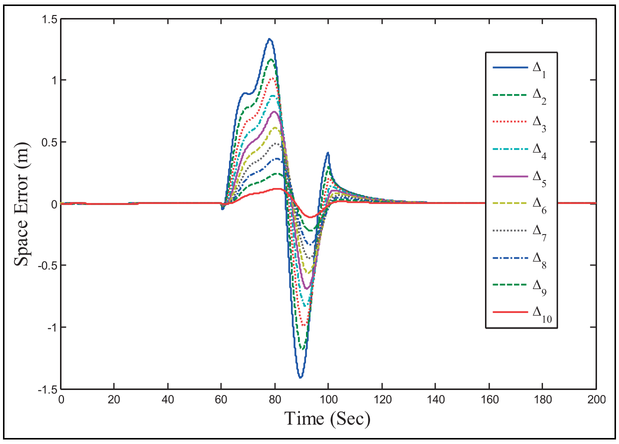

Figure 9. Performance of string stability under external disturbance.

internal stability, the control input is applied to all vehicles in platoon 7. Figure 8 depicts the spacing error and velocity of vehicles in this platoon. According to Figure 8(a), the spacing error decreases along the platoon indicating the string stability. Moreover, to evaluate the string stability of platoon 7 against external disturbance, the disturbance signal $d(t) = 4.56\sin(0.2t) + 2.31\cos(0.4t)$, $t \in [60, 100]$ is applied to leader of platoon 7. According to Figure 9, the string stability of this platoon is assured.

Conclusion

In this article, the control problem of homogeneous traffic flow by considering time delays was investigated based on CSS. The traffic flow consists of finite or infinite cooperative vehicular platoons. For inter-platoon control protocol, a new virtual leader-following consensus scheme was introduced. The inter-platoon closed-loop dynamics was decoupled to individual third-order dynamics. The stability analysis of the decoupled equations was performed based on Routh–Hurwitz and CTCR methods. Moreover, it was shown that this new scheme assures the inter-platoon string stability. It was assumed that the intra-platoon network topology is generic or even non-uniform. A new decoupling method was presented for intra-platoon closed-loop dynamics.

There are different works that can be addressed in future studies: (1) intra-platoon string stability analysis with generic network topology, (2) the modeling of leader-following scheme via Markov chain, and (3) the intra-platoon stability analysis of generic network topology in the presence of communication and data loss.

Declaration of conflicting interests

The author(s) declared no potential conflicts of interest with respect to the research, authorship, and/or publication of this article.

Funding

The author(s) received no financial support for the research, authorship, and/or publication of this article.

ORCID iD

Hossein Chehardoli http://orcid.org/0000-0002-6115-7429

References

1. Wang FY, Wang K, Lin W, et al. Data-driven intelligent transportation systems: a survey. *IEEE Trans Intell Transp Sys* 2011; 12(4): 1624–1639.
2. Li Y, Sun D, Liu W, et al. Modeling and simulation for microscopic traffic flow based on multiple headway, velocity and acceleration difference. *Nonlin Dynam* 2011; 66: 15–28.
3. Wang FY. Parallel control and management for intelligent transportation systems: concepts, architectures, and

applications. *IEEE Trans Intell Transp Sys* 2010; 11(3): 630–638.
4. Ge HX, Cheng RJ and Lei L. The theoretical analysis of the lattice hydrodynamic models for traffic flow theory. *Physica A* 2010; 389: 2825–2834.
5. Amoozadeha M, Deng H, Chuah CN, et al. Platoon management with cooperative adaptive cruise control enabled by VANET. *Vehicular Commun* 2015; 13: 110–123.
6. Santhana K and Rajamani R. On spacing policies for highway vehicle automation. *IEEE Trans Intell Transp Sys* 2003; 4(4): 198–204.
7. Jia D and Ngoduy D. Platoon based cooperative driving model with consideration of realistic inter-vehicle communication. *Trans Research Part C: Emerg Techn* 2016; l68: 245–264.
8. Santini S, Salvi A, Valente A, et al. A consensus-based approach for platooning with inter-vehicular communications and its validation in realistic scenarios. *IEEE Trans Veh Tech* 2016; 68(5): 423–435.
9. Li S, Zheng Y, Li K, et al. An overview of vehicular platoon control under the four component framework. In: *Proceedings of IEEE intelligent vehicles symposium*, Seoul, South Korea, 28 June–1 July 2015. New York: IEEE.
10. Chehardoli H and Homaeinezhad M. Stable control of a heterogeneous platoon of vehicles with switched interaction topology, time-varying communication delay and lag of actuator. *J Mech Eng Sci* 2017; 231(22): 4197–4208.
11. Ghasemi A, Kazemi R and Azadi S. Stable decentralized control of platoon of vehicles with heterogeneous information feedback. *IEEE Trans Veh Tech* 2013; 62: 4299–4308.
12. Naus GL, Vugts R, Ploeg J, et al. String-stable CACC design and experimental validation: a frequency-domain approach. *IEEE Trans Veh Tech* 2010; 59(9): 243–251.
13. Zheng Y, Eben S, Wang J, et al. Stability and scalability of homogeneous vehicular platoon: study on influence of information flow topologies. *IEEE Trans Intell Transp Sys* 2016; 17(1): 14–27.
14. Rajamani R. *Vehicle dynamics and control*. Berlin: Springer Science & Business Media, 2011.
15. Chehardoli H and Homaeinezhad MR. Third order safe consensus of heterogeneous vehicular platoons with MPF topology: constant time headway strategy. *J Automobile Eng*. Epub ahead of print 24 October 2017. DOI: 10.1177/0954407017725448.
16. Khatir M and Davidson E. Bounded stability and eventual string stability of a large platoon of vehicles using non-identical controllers. In: *Proceedings of the 43rd IEEE conference on decision and control (CDC)*, Nassau, Bahamas, 14–17 December 2004, pp. 135–141. New York: *IEEE*.
17. Ploeg J, Shukla DP, Wouw N, et al. Controller synthesis for string stability of vehicle platoons. *IEEE Trans Intell Transp Sys* 2014; 15(2): 854–865.
18. Bernardo M, Salvi A and Santini S. Distributed consensus strategy for platooning of vehicles in the presence of time-varying heterogeneous communication delays. *IEEE Trans Intell Transp Sys* 2015; 16(1): 102–112.
19. Chehardoli H and Homaeinezhad MR. Switching decentralized control of a platoon of vehicles with time-varying heterogeneous delay: a safe and dense spacing policy. *J Automobile Eng*. Epub ahead of print 23 September 2017. DOI: 10.1177/0954407017729309.
20. Middleton R and Braslavsky J. String instability in classes of linear time invariant formation control with limited communication range. *IEEE Trans Aut Control* 2010; 55: 1519–1530.
21. Ghasemi A, Kazemi R and Azadi S. Exact stability of a platoon of vehicles by considering time delay and lag. *J Mech Sci Techn* 2015; 29(2): 799–805.
22. Wang C and Nijmeijer H. String stable heterogeneous vehicle platoon using cooperative adaptive cruise control. In: *Proceedings of the IEEE 18th international conference on intelligent transportation systems (ITSC)*, Las Palmas, 15–18 September 2015. New York: *IEEE*.
23. Bernardo M, Falcone P, Salvi A, et al. Design, analysis, and experimental validation of a distributed protocol for platooning in the presence of time-varying heterogeneous delays. *IEEE Trans Control Sys Techn* 2016; 83(5): 237–251.
24. Peters AA, Middelton RH and Mason O. Leader tracking homogeneous platoons with broadcast delays. *Automatica* 2014; 50: 64–74.
25. Guo X, Wang J, Liao F, et al. Distributed adaptive integrated-sliding-mode controller synthesis for string stability of vehicle platoons. *IEEE Trans Intell Transp Sys* 2016; 17(9): 2419–2429.
26. Swaroop D, Hedrick K and Seibum B. Direct adaptive longitudinal control of vehicle platoons. *IEEE Trans Veh Techn* 2001; 50(1): 150–161.
27. Kwon JW and Chwa D. Adaptive bidirectional platoon control using a coupled sliding mode control method. *IEEE Trans Intell Transp Sys* 2014; 15(5): 2040–2048.
28. Ghasemi A and Rouhi S. A safe stable directional vehicular platoon. *Proc IMechE Part D: Jour of Automobile Eng* 2015; 229(8): 1083–1093.
29. Wu Y, Lu R, Shi P, et al. Adaptive output synchronization of heterogeneous network with an uncertain leader. *Automatica* 2017; 76: 183–192.
30. Wu Y, Lu R, Shi P, et al. An input-based triggering approach to leader-following problems. *Automatica* 2017; 75: 221–228.
31. Gu K, Kharitonov V and Chen J. *Stability of time-delay systems*. Basel: Birkhauser, 2003.
32. Ergenc AF, Ogac N and Fazalnia A. Extended Kronecker summation for cluster treatment of LTI systems with multiple delays. *Int J Control* 2007; 46(1): 143–155.
33. Seiler P, Pant A and Hedrick K. Disturbance propagation in vehicle strings. *IEEE Trans Automatic Control* 2004; 49(10): 1835–1841.
34. Zhang L and Orosz G. Motif-based design for connected vehicle systems in presence of heterogeneous connectivity structures and time delays. *IEEE Trans Intell Transp Sys* 2016; 17(1): 14–26.
35. Meyer CD. *Matrix analysis and applied linear algebra*. New York: Cambridge University Press, 2010.
36. Chehardoli H and Homaeinezhad MR. Robust control of a platoon of vehicles with communication time delay and switched interaction topology. *J Control* 2016; 10(3): 61–70.
37. Chehardoli H and Homaeinezhad MR. Control of a heterogeneous platoon of vehicles with actuator lag, communication delay and switched interaction topology: constant spacing and constant time headway policies. *J Control* 2017; 11(1): 27–37.

38. Salvi A, Santini S and Valente AS. Design, analysis and performance evaluation of a third order distributed protocol for platooning in the presence of time varying delays and switching topologies. *Transp Research Part C* 2017; 80: 360–383.
39. Qiu J, Wei Y, Karimi HR, et al. Reliable control of discrete-time piecewise-affine time-delay systems via output feedback. *IEEE Trans Reliability*. Epub ahead of print 20 September 2017. DOI: 10.1109/TR.2017.2749 242.
40. Wei Y, Qiu J, Karimi HR and Wang M. New results on H_inf dynamic output feedback control for Markovian jump systems with time-varying delay and defective mode information. *Optim Control App Meth* 2014; 35(6): 656–175.
41. Wei Y, Qiu J and Karimi HR. H_inf model reduction for continuous-time Markovian jump systems with incomplete statistics of mode information. *Int J Syst Sci* 2014; 45(7): 1496–1507.
42. Wei Y, Qiu J and Karimi HR. Quantized H_inf filtering for continuous-time Markovian jump systems with deficient mode information. *Asian J Control* 2015; 17(5): 1914–1923.
43. Zhang H and Wang J. Active steering actuator fault detection for an automatically-steered electric ground vehicle. *IEEE Trans Veh Techn* 2017; 66(5): 3685–3702.
44. Zhang H and Wang J. Adaptive sliding-mode observer design for a selective catalytic reduction system of ground-vehicle diesel engines. *ASME/IEEE Trans Mechat* 2016; 21(4): 2027–2038.
45. Chehardoli H and Ghasemi A. Adaptive robust output tracking control of uncertain nonlinear cascade systems with disturbance and multiple unknown time-varying delays. *Asian J Control* 2017; 19: 2009–2016.
46. Chehardoli H and Eghtesad M. Robust adaptive control of switched nonlinear systems in strict feedback form with unknown time delay. *IMA J Math Control Inf* 2015; 32: 761–779.

Appendix 1

Proof of theorem 3

A non-singular matrix $\tilde{\mathbf{V}}$ can be found such that

$$\tilde{\mathbf{V}}^{-1}\mathbf{H}\tilde{\mathbf{V}} = \tilde{\Xi},\ \tilde{\boldsymbol{\Xi}} = diag\{\tilde{\boldsymbol{\Xi}}_1, ..., \tilde{\boldsymbol{\Xi}}_n, \tilde{\boldsymbol{\Xi}}_{n+1}, \tilde{\boldsymbol{\Xi}}^*_{n+1}, ..., \tilde{\boldsymbol{\Xi}}_{n+m}, \tilde{\boldsymbol{\Xi}}^*_{n+m}\} \tag{49}$$

where $\tilde{\boldsymbol{\Xi}}_i$, $i = 1, \ldots, n$ is in the form of equation (38); $\tilde{\boldsymbol{\Xi}}_i$, $i = n+1, \ldots, n+m$ is in the form of equation (39); and (*) denotes the complex conjugate operator. Also, $\tilde{\mathbf{V}}$ is in the following form

$$\tilde{\mathbf{V}} = \left(\tilde{\mathbf{V}}_1, \tilde{\mathbf{V}}_2, \ldots, \tilde{\mathbf{V}}_{n+m}\right) \tag{50}$$

For real eigenvalues, $\tilde{\mathbf{W}}_i \in \Re^{N\times n_i}$, $i = 1, 2, \ldots, n$ and for complex eigenvalues, $\tilde{\mathbf{V}}_i \in \Re^{N\times m_i}$, $i = n+1, \ldots, n+m$. For $n+1 \leqslant r \leqslant n+m$, we have the following

$$\mathbf{H}\tilde{\mathbf{V}}_r = \tilde{\mathbf{V}}_r\tilde{\boldsymbol{\Xi}}_r,\ \mathbf{H}\tilde{\mathbf{V}}^*_r = \tilde{\mathbf{V}}^*_r\tilde{\boldsymbol{\Xi}}^*_r \tag{51}$$

$\tilde{\mathbf{V}}_r$ can be expressed as $\tilde{\mathbf{V}}_r = (\mathbf{v}_{r1}, \mathbf{v}_{r2}, \ldots, \mathbf{v}_{rn_r})$. $\mathbf{v}_{rk}$ is as follows

$$\mathbf{v}_{rk} = \bar{\mathbf{v}}_{rk} + j\tilde{\mathbf{v}}_{rk},\ 1 \leqslant k \leqslant n_r; \bar{\mathbf{v}}_{rk}, \tilde{\mathbf{v}}_{rk} \in \Re^N \tag{52}$$

Using equation (51) for $k = 1$, we have the following

$$\mathbf{H}\mathbf{v}_{r1} = \bar{\varepsilon}_r\mathbf{v}_{r1} \tag{53}$$

Applying equation (52) in equation (53) leads to the following

$$\begin{aligned}\mathbf{H}\mathbf{v}_{r1} &= (p_r + jq_r)(\bar{\mathbf{v}}_{r1} + j\tilde{\mathbf{v}}_{r1}) \\ &= (p_r\bar{\mathbf{v}}_{r1} - q_r\tilde{\mathbf{v}}_{r1}) + j(p_r\tilde{\mathbf{v}}_{r1} + q_r\bar{\mathbf{v}}_{r1})\end{aligned} \tag{54}$$

Equation (54) can be divided into the following equations

$$\mathbf{H}\bar{\mathbf{v}}_{r1} = p_r\bar{\mathbf{v}}_{r1} - q_r\tilde{\mathbf{v}}_{r1},\ \mathbf{H}\tilde{\mathbf{v}}_{r1} = p_r\tilde{\mathbf{v}}_{r1} + q_r\bar{\mathbf{v}}_{r1} \tag{55}$$

Equation (55) is equivalent to the following

$$\mathbf{H}[\bar{\mathbf{v}}_{r1}\tilde{\mathbf{v}}_{r1}] = [\bar{\mathbf{v}}_{r1}\tilde{\mathbf{v}}_{r1}]\begin{bmatrix} p_r & q_r \\ -q_r & p_r \end{bmatrix} = [\bar{\mathbf{v}}_{r1}\tilde{\mathbf{v}}_{r1}]\boldsymbol{\Xi}_r \tag{56}$$

For $1 < k \leqslant n_r$, it can be written that

$$\mathbf{H}\mathbf{v}_{rk} = \bar{\varepsilon}_r\mathbf{v}_{rk} + \mathbf{v}_{r(k-1)} \tag{57}$$

Replacing equation (52) in equation (57) will result in the following

$$\begin{aligned}\mathbf{H}\mathbf{v}_{rk} = \mathbf{H}(\bar{\mathbf{v}}_{rk} + j\tilde{\mathbf{v}}_{rk}) &= \left(p_r\bar{\mathbf{v}}_{rk} - q_r\tilde{\mathbf{v}}_{rk} + \bar{\mathbf{v}}_{r(k-1)}\right) \\ &+ j\left(p_r\tilde{\mathbf{v}}_{rk} + q_r\bar{\mathbf{v}}_{rk} + \tilde{\mathbf{v}}_{r(k-1)}\right)\end{aligned} \tag{58}$$

In matrix form, equation (58) can be written as follows

$$\begin{aligned}\mathbf{H}[\bar{\mathbf{v}}_{rk}\tilde{\mathbf{v}}_{rk}] &= \left[\bar{\mathbf{v}}_{r(k-1)}\tilde{\mathbf{v}}_{r(k-1)}\bar{\mathbf{v}}_{rk}\tilde{\mathbf{v}}_{rk}\right]\begin{bmatrix} 1 & 0 & p_r & -q_r \\ 0 & 1 & q_r & p_r \end{bmatrix}^T \\ &= \left[\bar{\mathbf{v}}_{r(k-1)}\tilde{\mathbf{v}}_{r(k-1)}\bar{\mathbf{v}}_{rk}\tilde{\mathbf{v}}_{rk}\right]\begin{bmatrix} \mathbf{I}_2 & \boldsymbol{\Xi}_r \end{bmatrix}^T\end{aligned} \tag{59}$$

Therefore, for rth eigenvalue with repetition order n_r, the matrix $\mathbf{w}_r$ will be in the following form

$$\mathbf{v}_r = [\bar{\mathbf{v}}_{r1}, \tilde{\mathbf{v}}_{r1}, \bar{\mathbf{v}}_{r2}, \tilde{\mathbf{v}}_{r2}, \ldots, \bar{\mathbf{v}}_{rn_r}, \tilde{\mathbf{v}}_{rn_r}] \tag{60}$$

So that we can write as follows

$$\mathbf{H}\mathbf{v}_r = \mathbf{v}_r\boldsymbol{\Xi}_r \tag{61}$$

where $\boldsymbol{\Xi}_r$ is defined in equation (39). In continuance of the proof, matrix $\mathbf{V} \in \Re^{N\times N}$ is defined as follows

$$\mathbf{V} = \left[\tilde{\mathbf{V}}_1, \ldots, \tilde{\mathbf{V}}_n, \mathbf{V}_{n+1}, \ldots, \mathbf{V}_{n+m}\right] \tag{62}$$

In equation (62), the first n blocks are corresponding to real eigenvalues, and other blocks following equation (60) are corresponding to complex eigenvalues. Now, we can write that

$$\mathbf{HV} = \mathbf{V}\boldsymbol{\Xi} \tag{63}$$

Finally, the non-singularity of $\mathbf{V}$ should be proven. For imaginary eigenvalues, we can write that

$$\bar{\mathbf{v}}_{rk} = \frac{\mathbf{v}_{rk} + \mathbf{v}_{rk}^*}{2}, \ \tilde{\mathbf{v}}_{rk} = \frac{\mathbf{v}_{rk} - \mathbf{v}_{rk}^*}{2} \tag{64}$$

We define the matrix $\mathbf{X} = 1/2(diag\{X_1, X_2, \ldots, X_{n+m}\})$ where

$$X_i = 2, \ i = 1, 2, \ldots, n; \quad X_i = \begin{bmatrix} 1 & 1 \\ 1 & -1 \end{bmatrix}, \quad i = n+1, \ldots, n+m \tag{65}$$

Now, we can write $\mathbf{V} = \tilde{\mathbf{V}}\mathbf{X}$. Since the matrices $\mathbf{X}$ and $\tilde{\mathbf{V}}$ are non-singular, it is inferred that $\mathbf{V}$ is also non-singular. So that from equation (63), we have the following

$$\mathbf{V}^{-1}\mathbf{H}\mathbf{V} = \mathbf{\Xi} \tag{66}$$

and the proof is complete.

Appendix 2

Mathematical lemmas

Lemma 1.[8,10] The matrix $\mathbf{H}$ is positive definite if the lead vehicle is globally reachable in $\bar{G}$.

Lemma 2.[45,46] For any vectors $\mathbf{a}$, $\mathbf{b}$ and any positive definite matrix $\boldsymbol{\varsigma}$, the inequality $2\mathbf{a}^T\mathbf{b} \leqslant \mathbf{a}^T\boldsymbol{\varsigma}\mathbf{a} + \mathbf{b}^T\boldsymbol{\varsigma}^{-1}\mathbf{b}$ holds.

Lemma 3.[31] An arbitrary matrix $\mathbf{A}$ is asymptotically stable if there exists a positive definite matrix $\mathbf{P}$ satisfying $\mathbf{AP} + \mathbf{PA}^T < \mathbf{0}$.

Lemma 4.[31] The sum of two definite and semi-definite matrices is a definite matrix.

Lemma 5.[35,36] For arbitrary matrices $\mathbf{M}_1, \mathbf{M}_2, \mathbf{M}_3, \mathbf{M}_4$ with appropriate dimensions, the equality $(\mathbf{M}_1 \otimes \mathbf{M}_2)(\mathbf{M}_3 \otimes \mathbf{M}_4) = (\mathbf{M}_1\mathbf{M}_3) \otimes (\mathbf{M}_2\mathbf{M}_4)$ holds, where $\otimes$ is the Kronecker product.